# SINTERING OF BULK HIGH-T$_c$ SUPERCONDUCTORS: Y–Ba–Cu–O*

K. C. Goretta, Nan Chen, M. T. Lanagan, W. Wu,
J. P. Singh, R. A. Olson, J. L. Routbort, and R. B. Poeppel

Argonne National Laboratory
Argonne, IL 60439

ANL/CP--74238

DE92 016190

May 1992

## DISCLAIMER

Paper submitted for publication in Proceedings of 1992 Powder Metallurgy World Congress, June 21–26, 1992, San Francisco, CA.

# SINTERING OF BULK HIGH–$T_c$ SUPERCONDUCTORS: Y–Ba–Cu–O

K. C. Goretta, Nan Chen, M. T. Lanagan, W. Wu,
J. P. Singh, R. A. Olson, J. L. Routbort, and R. B. Poeppel

Argonne National Laboratory
Argonne, IL 60439

## ABSTRACT

Sintering of bulk $YBa_2Cu_3O_x$ (123) samples has been conducted from 850 to 1010°C in oxygen partial pressures ($P_{O_2}$) of 2.5 x $10^2$ to $10^5$ Pa. The final grain sizes of the samples were controlled by selective use of (1) liquid phases and (2) partial decomposition of the 123 phase by sintering in a $P_{O_2}$ that was lower than the minimum needed for 123 stability. In nearly fully dense samples, it was found that the grain size could range from about 1 to 500 μm, depending on the processing conditions.

## INTRODUCTION

The Y–Ba–Cu–O system contains three superconducting phases: $YBa_2Cu_3O_x$ (123), $YBa_2Cu_4O_y$ (124), and $YBa_2Cu_{3.5}O_z$ (247). The 123 phase was discovered first. It has the highest superconducting transition temperature of the three (90–100 K) and is the easiest to consolidate [1-3]. It has, therefore, been the most extensively studied. 123 has an orthorhombic crystal structure in which a ≈ b and the c axis is approximately triple the a or b axis [1].

Sintering of 123 can be very difficult to accomplish because of the very slow diffusion rates of Y and Ba [4-6]. In addition, diffusion in 123 is highly anisotropic. For the species that have been measured, the diffusion coefficients in the c direction are $10^2 - 10^6$ times slower than in the a–b plane [4-7]. This pronounced anisotropy affects microstructural development strongly.

There are several considerations that will influence the final density and grain size of 123. The first consideration is melting. The 123 phase undergoes peritectic melting in $O_2$ at about 1025°C. This temperature decreases significantly with decreasing $P_{O_2}$ [8,9]. Slow cooling from the melt can be used to grow very large 123 grains [10]. Slow solidification in a temperature gradient can cause the grains to align preferentially [11]. Reviews of melt–processing of 123 can be found in Refs. 12 and 13.

*/*

Many 123 sintering studies have been published. Effects of processing atmosphere [14-17], second phases [18-21], and method of heating [22] have been examined. The studies have been conducted on powders of differing phase purities and particle size, shape, and distribution. As a consequence, it can be very difficult to compare results directly. This work will include a summary of our previous work on sintering of 123, for which we have consistent powders, and new results on direct control of grain growth.

The key features of this work are the control of $P_{O_2}$ and selective use of transient liquids. In the $P_{O_2}$ range of this study, $2 \times 10^2$ to $10^5$ Pa, the melting point of 123 decreases 65–70°C with the $P_{O_2}$ decrease [14]. Our work was restricted to temperatures at which 123 was solid. It has been well documented that eutectics of 123–CuO–$BaCuO_2$ melt at temperatures 80–130°C lower than 123 itself melts [8,14]. Thus, the presence of CuO and $BaCuO_2$ can lead to rapid liquid–phase sintering at relatively low temperatures [20,23,24]. In addition, sintering, creep, and diffusional data indicate that solid–state diffusional kinetics in 123 increase with decreasing $P_{O_2}$ [4,5,14,25,26]. As a final consideration, if the $P_{O_2}$ is too low, the 123 phase will begin to decompose [27]. It will be shown that this decomposition can be used to one's advantage.

## EXPERIMENTS

The 123 powder used in most of the experiments was synthesized from reagent–grade $Y_2O_3$, $BaCO_3$, and CuO. The starting powders were weighed to the correct cation stoichiometry and placed in a polyethylene jar containing methyl alcohol and $ZrO_2$ grinding media. The mixture was ball milled for 16 h and dried. The dry powder was screened through a 30–mesh sieve and calcined at 800°C for 4 h in flowing $O_2$ at a pressure of $2.6 \times 10^2$ Pa. Final grinding yielded an average particle size of 4 μm. The powder was phase pure by X–ray diffraction and differential thermal analysis [28].

For a few of the older studies, the 123 powder was heat treated differently. The dry powder was pressed at a pressure of 140 MPa into a series of 80-g, 44–mm–diameter pellets that were placed on MgO single crystals and heated in air to 890°C for 24 h. The pellets were then cooled, crushed, and ground in a tungsten carbide rotary mill. The resultant powder was pressed into pellets, fired in air at 890°C for 24 h, and ground two additional times. Final grinding in a jet mill yielded an average particle size of 2.5 μm. Slight traces of $BaCuO_2$ and $Y_2BaCuO_5$ were present [14,19].

The powders were pressed into a series of small pellets and heat treated under a variety of conditions. The temperature range was 850–1010°C, the $P_{O_2}$ range was $2 \times 10^2$–$10^5$ Pa, and the time range was 1–250 h. The densities of the resultant pellets were measured geometrically. The microstructures and phase contents were examined by X–ray diffraction, differential thermal analysis (DTA), optical microscopy, and scanning electron microscopy (SEM).

## RESULTS

Either pure or impure powders have been used in all 123 sintering studies. Many powders contain appreciable concentrations of impurity phases such as CuO, $BaCuO_2$, and $Y_2BaCuO_5$. Higher quality powders contain little or none of these phases [28]. As shown in Fig. 1, the more–pure powders melt at about 1025°C in $O_2$ and the less–pure powders contain phases that melt at lower
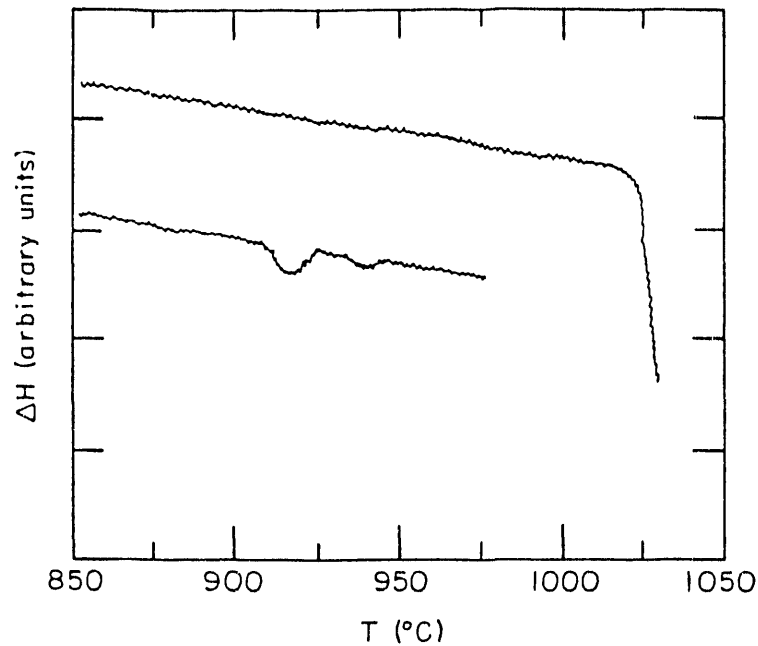
Figure 1. Differential thermal analysis plots of pure 123 powder (top) and powder containing impurity phases (bottom) heated in $O_2$ at 5°C/min.

temperatures. The final microstructure of a sintered compact will depend on which type of powder was used.

It is clear from Fig. 1 that a range of temperatures exists for impure powders in which 123 is solid and substantial liquid is present. This liquid can be used to promote densification and grain growth. As shown in Fig. 2, densification kinetics increase with decreasing $P_{O_2}$ and, more dramatically, once a liquid phase is formed, as for 0.2% $O_2$ in the figure, the kinetics become very rapid.
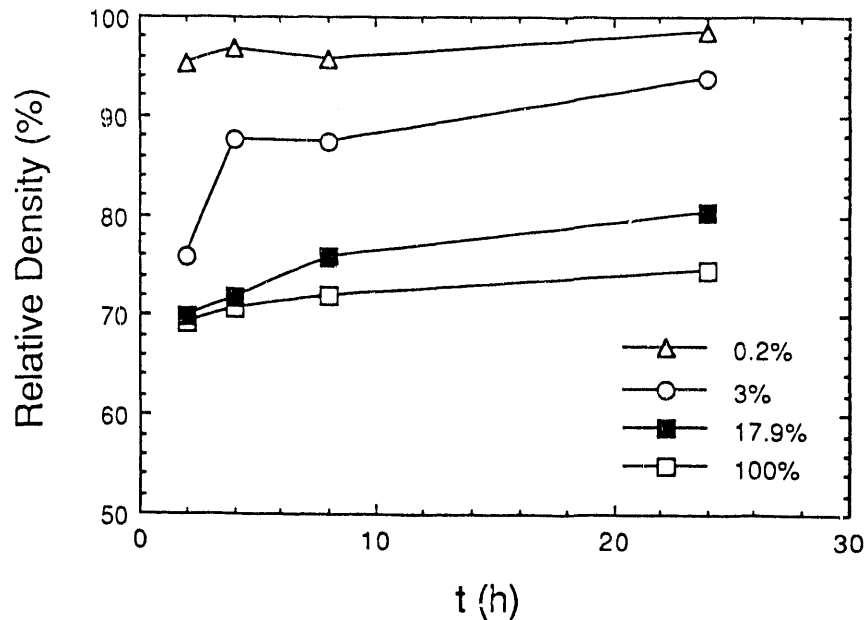


Figure 2. Density versus time for 123 pellets sintered at 890°C in the $O_2$ percentages shown; the 123 was not phase pure (see Fig. 1).

Although eutectic liquids improve densification, it has generally been observed that the CuO–BaCuO₂ types of liquids solidify along grain boundaries and severely degrade superconducting properties [19,23]. If the starting 123 powder is stoichiometric, then it is possible to perform a post–sintering anneal to cause the grain boundary phases to react to form 123. It has been shown that anneals in $O_2$ at intermediate temperatures of about 800–860°C for times of 3–10 days can cause the extraneous phases to react to 123 [23]. This reaction has been confirmed by SEM and DTA. Thus, one may take advantage of the enhanced kinetics of liquid–phase sintering, and through use of a post–sintering anneal, remove many of the deleterious effects of the liquid.
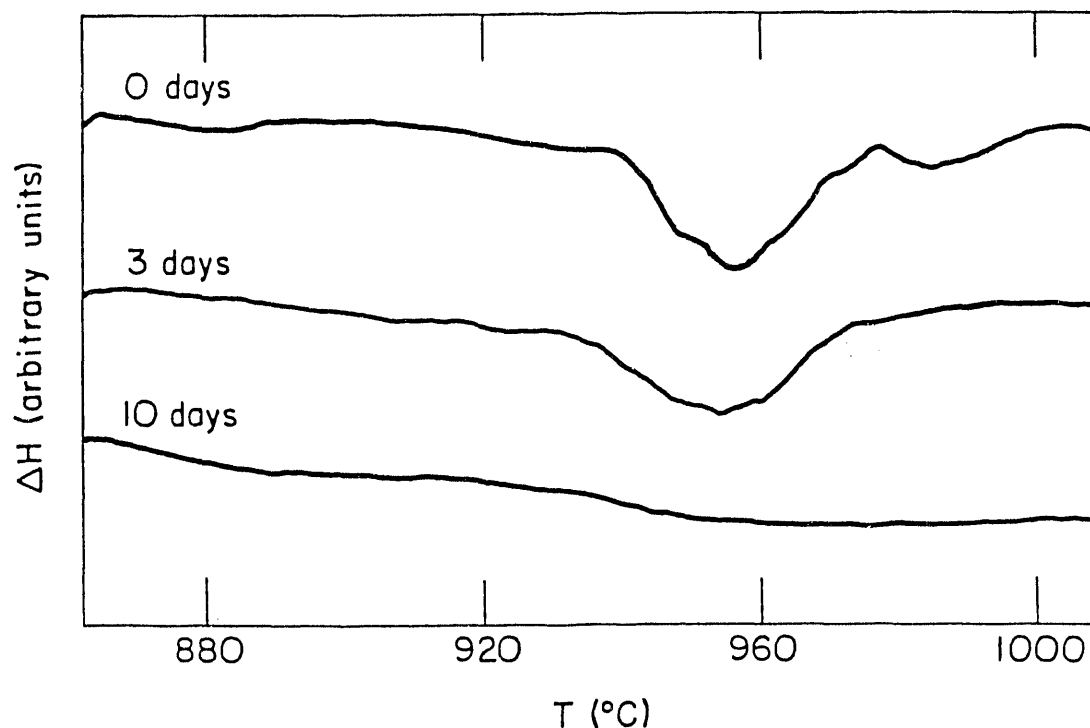


Figure 3. DTA traces of 123 pellets after sintering and annealing; the endotherms associated with second phases that are present before the extended anneals are absent after 10 days.

Eutectic liquids also induce grain growth during sintering. In the absence of such liquids, grain growth in 123 is substantially reduced [14,20,23,24,29,30]. Representative densification and grain growth data for 123 sintered in $O_2$ are shown in Figs. 4 and 5. The 123 powder used in these studies was highly pure [28], but the rapid initial increase in density from 930 to 990°C indicates that some liquid phase was present initially at those temperatures. Microstructures of pellets sintered for 24 h are shown in Fig. 6. The data and SEM indicate that little densification or increase in grain length occurred after an initial short period. As the temperature increased, however, grain growth occurred, primarily through grains becoming thicker rather than longer. The sequence of growth appears to have been an initial increase in length along the a–b planes, as would be expected from diffusion data [4-7], at which point the larger grains impinged upon each other. Subsequent growth occurred by consumption of smaller grains within regions surrounded by larger grains through thickening of the larger grains. It is noted that the grain growth was sufficiently rapid to trap large amounts of porosity

4

within the grains. The concentration of intragranular porosity was smallest for the samples sintered at 900°C, which also had the slowest rates of grain growth.

Had the 123 powder been less pure, more liquid would have been present during sintering, and the grains would have become much longer [14,20,23]. The aspect ratios would also have been larger. Had the powder been more pure, the amounts of intragranular porosity would have been less and the times needed to induce densification would have been longer.
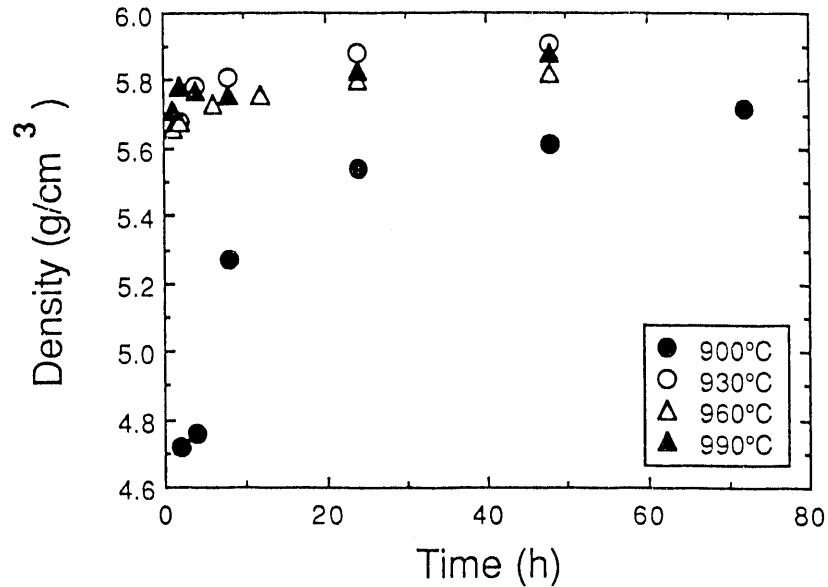


Figure 4. Density versus sintering time for 123 heat treated in $O_2$ at the temperatures shown; the theoretical density is 6.3 g/cm$^3$ [1].
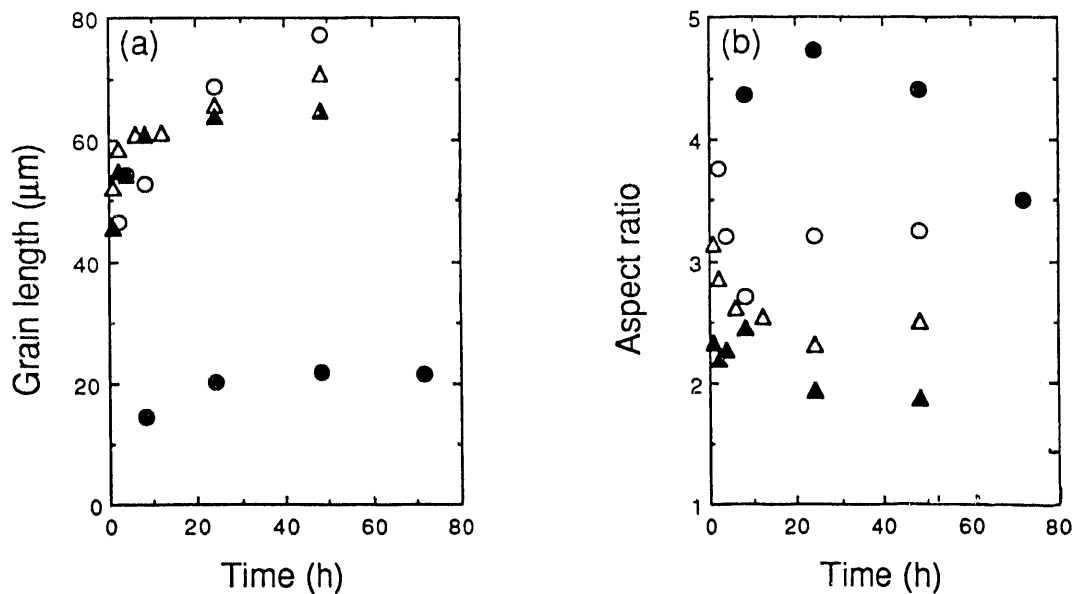


Figure 5. Data for the 50 largest grains in each image obtained by SEM: (a) average grain length and (b) average aspect ratio for sintering at the following temperatures: 900°C (filled circles), 930°C (open circles), 960°C (open triangles), and 990°C (filled triangles).
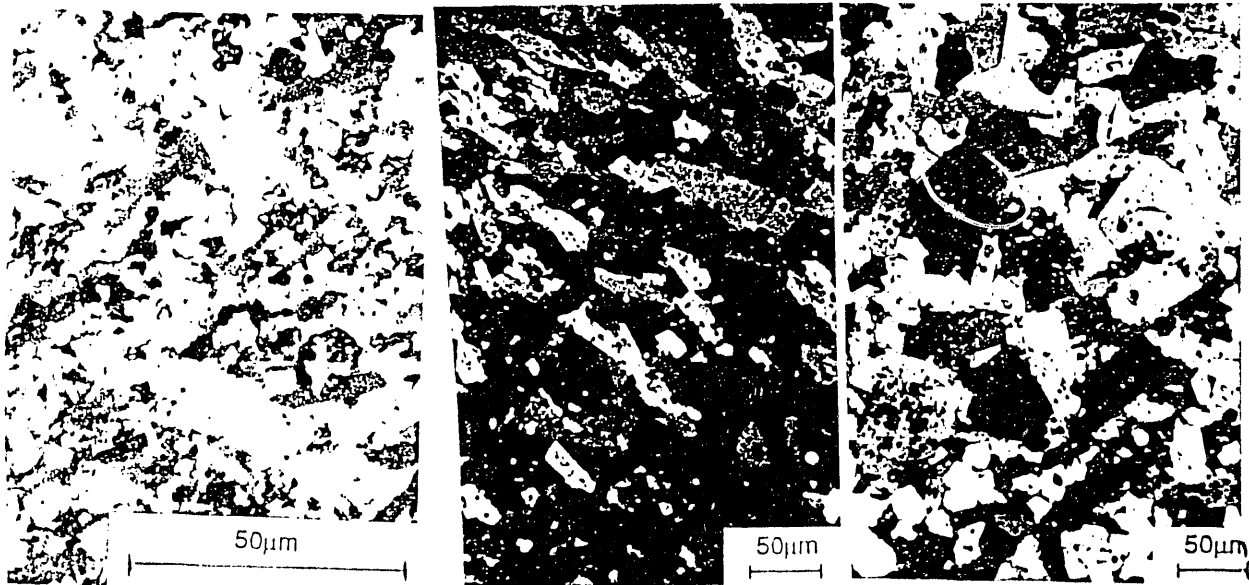
Figure 6.   Optical photomicrographs of 123 sintered in $O_2$ for 24 h at (a) 900°C, (b) 930°C, and (c) 990°C.

Complete avoidance of $CuO-BaCuO_2$ liquids could have reduced the grain sizes substantially. It is very difficult, however, to eliminate them completely from 123 powders. These eutectic liquids also come into play when $P_{O_2}$ is selectively manipulated to control grain size. The principal consideration for changing the atmosphere during sintering is shown in Fig. 7. If the $P_{O_2}$ becomes too low, 123 begin decomposes. Comparison of Figs. 1 and 7 reveals that for nearly pure powders, the decomposition of 123 occurs in the solid state; for impure powders, liquids form during the decomposition.
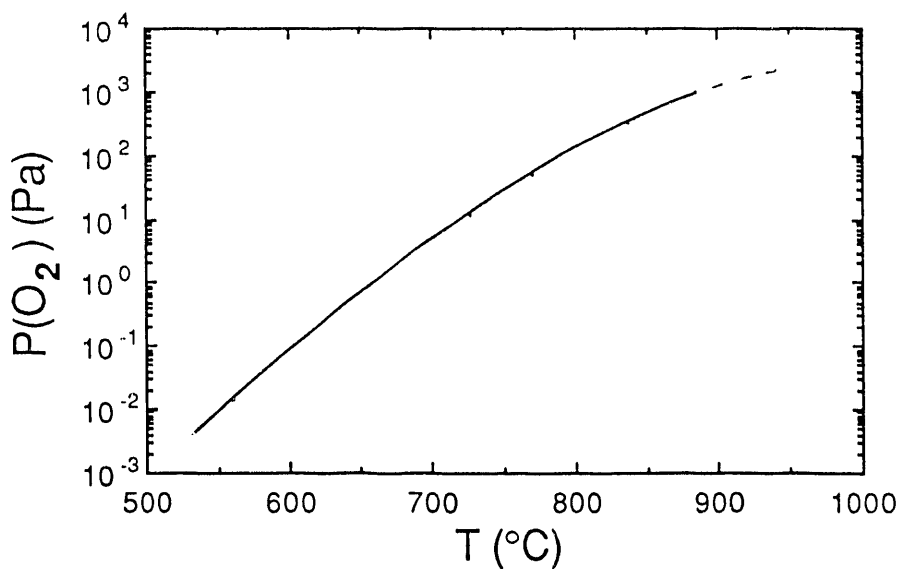


Figure 7.   Stability range for 123 as a function of temperature and $P_{O_2}$; data taken from [27].

The solid–state decomposition products are principally $Cu_2O$ and $Y_2BaCuO_5$, which are very fine grain–boundary phases. During sintering, they act to pin grain growth. As a consequence, 123 can be sintered to nearly 100% density without undergoing appreciable grain growth. Fine grained, very strong products result. For example, extruded wires sintered in 1% $O_2$ at 910°C have achieved densities greater than 90% of theoretical and strengths of about 200 MPa [31]. Recently, the strengths of wires sintered in 0.2% $O_2$ at 900°C have reached 230 MPa. Furthermore, post–sintering anneals in $O_2$ can convert the decomposition products to 123 without inducing appreciable grain growth. It was found that the grain size of a compact that was sintered in 1% $O_2$ at 910°C, which is in the decomposition range, was approximately that of the starting powder. X–ray diffraction revealed that the compact contained measurable amounts of $Cu_2O$ and $Y_2BaCuO_5$. Annealing in $O_2$ at 845°C for 24 h caused sufficient formation of the 123 phase such that no extraneous phases could be detected by X–ray diffraction. This anneal did not induce grain growth. The result was a highly pure, fine–grained product.

When a $CuO–BaCuO_2$ eutectic were present during the decomposition heat treatment, larger, plate–like grains resulted. The post–sintering anneal at 845°C did not produce measurable improvements in phase purity. For example, it was found for some Cu–excess 123 powders that the anneals caused the CuO, which had been present along grain boundaries, to migrate from the grain boundaries to form large, discrete phases (Fig. 8). For reaction to form 123 during the post–sintering anneal, it is essential that the phases that form during the decomposition heat treatment be present as fine grain–boundary phases. Coarse phases, gross segregation of some species, or wholesale nonstoichiometry can prevent complete conversion to the desired 123 phase.
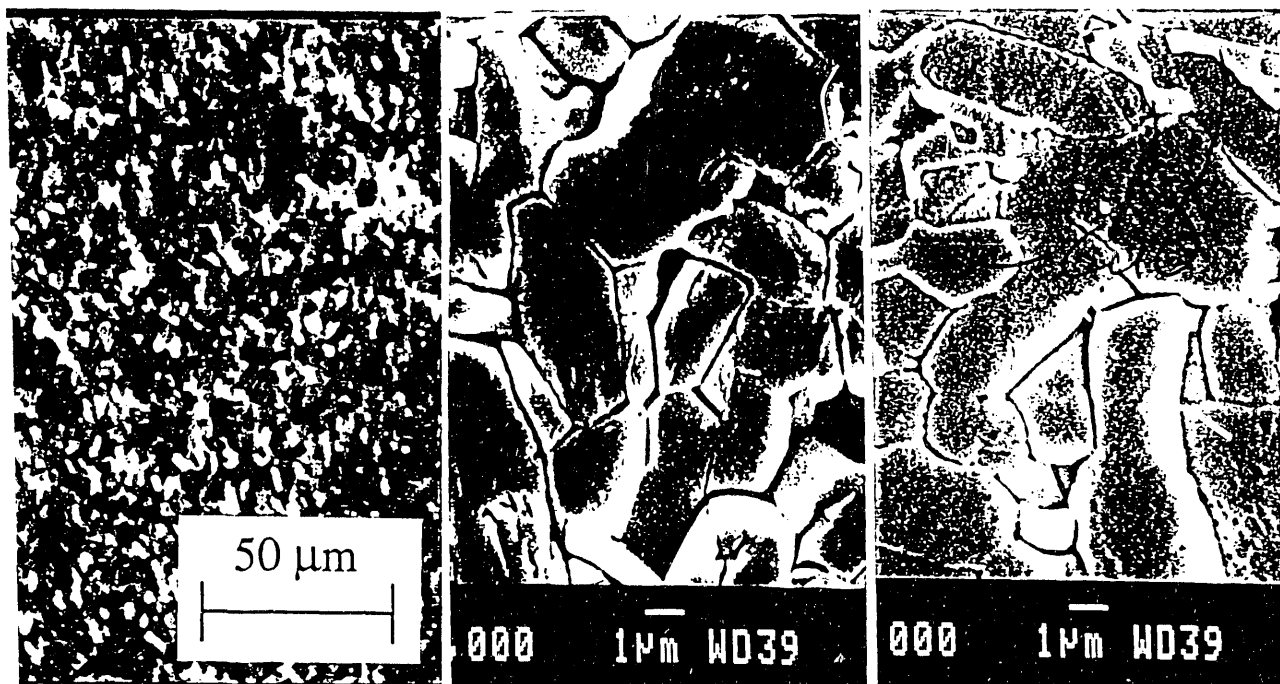


Figure 8. Photomicrographs of 123 sintered in 1% $O_2$ at 910°C: (a) optical image of powder of good phase purity after a 24–h anneal at 845°C; (b) SEM image of Cu–excess powder prior to post–sintering anneal; and (c) SEM image of Cu–excess powder after 24 anneal in which the CuO phase can be clearly seen.

## SUMMARY

The selective manipulation of decomposition, control of liquid phases, and choice of post–sintering annealing conditions to cause the 123 phase to reform constitute a comprehensive scheme for control of 123 densification and grain size. In most cases, the grain size of 123 can be tailored to the application by controlling temperature, $P_{O_2}$, time, and powder purity. In addition, the use of decomposition/recomposition heat treatments is not restricted to the 123 system. Any complex oxide that can be made to partially decompose in low $P_{O_2}$ in the solid state can be similarly processed. Strong, fine–grained products of good phase purity wi'l result.

## REFERENCES

1. R. Beyers and T. M. Shaw, Sol. State Phys., **42** (1989) 135–212.
2. D. E. Morris, A. G. Markelz, B. Fayn, and J. H. Nickel, Physica C, **168** (1990) 153–160.
3. R. K. Williams, J. Brynestad, T. J. Henson, D. M. Kroeger, G. C. Marsh, R. A. Padgett, and J. O. Scarbrough, J. Appl. Phys., **69** (1991) 2426–2430.
4. N. Chen, Ph.D. Thesis, Illinois Institute of Technology, 1991.
5. J. L. Routbort, N. Chen, K. C. Goretta, and S. J. Rothman, in *High–Temperature Superconductors: Materials Aspects*, H. C. Freyhardt, R. Flükiger, and M. Peuckert, eds. (Oberursel, Germany: DGM Informationsgesellschaft, 1991) pp. 569–579.
6. J. L. Routbort, S. J. Rothman, N. Chen, J. N. Mundy, and J. E. Baker, Phys. Rev. B, **43** (1991) 5489–5497.
7. S. J. Rothman, J. L. Routbort, U. Welp, and J. E. Baker, Phys. Rev. B, **44** (1991) 2326–2333.
8. T. Aselage and K. Keefer, J. Mater. Res., **3** (1988) 1279–1291.
9. K. W. Lay and G. M. Renlund, J. Am. Ceram. Soc., **73** (1990) 1208–1210.
10. S. Kuharuangrong and J. Taylor, J. Am. Ceram. Soc., **74** (1991) 1964–1969.
11. S. Jin, T. H. Tiefel, R. C. Sherwood, R. B. van Dover, M. E. davis, G. W. Kammlott, and R. A. Fastnacht, Phys. Rev. B, **37** (1988) 7850–7853.
12. S. Jin and J. E. Graebner, Mater. Sci. Eng., **B7** (1991) 243–260.
13. P. J. McGinn, W. Chen, and N. Zhu, J. Met., **43** [3] (1991) 26–28.
14. N. Chen, D. Shi, and K. C. Goretta, J. Appl. Phys., **66** (1989) 2485–2488.
15. Y. Gao, Y. Li, K. L. Merkle, J. N. Mundy, C. Zhang, U. Balachandran, and R. B. Poeppel, Mater. Lett., **9** (1990) 347–352.
16. S. E. Dorris, K. C. Goretta, B. Hajyousif, U. Balachandran, J. T. Dusek, D. Shi, and R. B. Poeppel, Ceram. Trans., **13** (1990) 381–387.
17. E. H. Lee, J. Y. Jeong, H. I. Song, and S.–Y. Yoon, Jpn. J. Appl. Phys., **30** (1991) L1092–1095.
18. T. Itoh and H. Uchikawa, J. Appl. Phys., **66** (1989) 4900–4902.

19. I. Bloom, B. S. Tani, M. C. Hash, D. Shi, M. A. Patel, K. C. Goretta, N. Chen, and D. W. Capone II, J. Mater. Res., **4** (1989) 1093–1098.
20. L. C. Stearns, M. P. Harmer, and H. C. Chan, J. Am. Ceram. Soc., **73** (1990) 2740–2742.
21. L. C. Stearns, M. P. Harmer, and H. C. Chan, J. Am. Ceram. Soc., **74** (1991) 2175–2179.
22. H.-E. Kim, H. D. Kimrey, and D. J. Kim, J. Mater. Sci. Lett., **10** (1991) 742–744.
23. D. Shi, D. W. Capone II, G. T. Goudey, J. P. Singh, N. J. Zaluzec, and K. C. Goretta, Mater. Lett., **6** (1988) 217–221.
24. K. No, J. D. Verhoeven, R. W. McCallum, and E. D. Gibson, IEEE Trans. Magn., **25** (1989) 2184–2187.
25. K. C. Goretta, R. B. Poeppel, D. Shi, N. Chen, S. J. Rothman, J. L. Routbort, and J. P. Stoessel, Ceram. Trans., **13** (1990) 369–379.
26. K. C. Goretta, J. L. Routbort, A. C. Biondo, Y. Gao, A. R. de Arellano–López, and A. Dominguez–Rodriguez, J. Mater. Res., **5** (1990) 2766–2770.
27. R. Bormann and J. Nölting, Appl. Phys. Lett., **54** (1989) 2148–2150.
28. U. Balachandran, R. B. Poeppel, J. E. Emerson, S. A. Johnson, M. T. Lanagan, C. A. Youngdahl, D. Shi, K. C. Goretta, and N. G. Eror, Mater. Lett., **8** (1989) 454–456.
29. A. H. Hamdi, J. V. Mantese, A. L. Micheli, R. A. Waldo, Y. L. Chen, and C. A. Wong, Appl. Phys. Lett., **53** (1988) 435–437.
30. L. Martinez, L. Vazquez, J. L. Albarran, J. Fuentes, E. Carrillo, A. Mendoza, E. Orozco, J. G. Ferez–Ramirez, R. Perez, L. Cota, J. L. Boldu, and M. J. Yacaman, Mater. Sci. Eng., **A110** (1989) 217–221.
31. J. P. Singh, J. Joo, R. Guttschow, and R. B. Poeppel, in Proceedings of 1992 Texas Center for Superconductivity Workshop on High–Temperature Superconducting Materials, Houston, TX, February 27, 1992, in press.

# DATE FILMED

8 / 11 / 92